Bull. Astr. Soc. India (2000) **28**, 225-232

Mid-and far-infrared studies of galactic compact H II regions

S.K. Ghosh

Tata Institute of Fundamental Research, Homi Bhabha Road, Mumbai 400 005, India

Abstract. Several Galactic H II region complexes have been observed in the far infrared (FIR) wavebands using the TIFR 1-m balloon borne telescope, and in the mid infrared (MIR) using the Infrared Space Observatory (ISO). Many of these FIR maps show interesting structural details. The MIR observations have clearly detected PAH features in two compact H II regions and one molecular clump. A self consistent radiative transfer scheme (1-D) has been developed which has been successful in extracting important details like geometric sizes, radial density distribution, dust composition, etc, from these and other similar measurements.

A new scheme (2-D) has been developed in cylindrical geometry to model IRAS 19181 + 1349, which has been resolved into two sources. The model parameters in this scheme have been constrained by the observed spectral energy distribution (SED) and radial profiles at MIR & FIR wavebands.

Non-equilibrium processes have also been incorporated in spherical geometry, to explain the PAH emission features. This scheme has successfully explained high resolution spectra (ISO-SWS) of several Galactic compact H II regions.

1 Observations

A far infrared (FIR) astronomy programme is being pursued using the TIFR 100 cm balloon borne telescope (Ghosh et al. 1988), with the aim of understanding the energetics, spatial density & temperature distribution of dust in Galactic star forming regions (SFR). Two main features of this FIR programme are : trans-IRAS wavebands ($\lambda > 100$ μm) to complement the IRAS & for detecting cooler dust (< 20 K); and high angular resolution. Near diffraction limited (≈ 1') maps are generated in two FIR bands ($\lambda_{eff} \approx 143$ & 185 μm) from simultaneous measurements using a 12 channel photometer system (Verma et al. 1993). The Galactic SFRs observed using this system (1993-98) are listed along with some observational details in Table 1. Many of these sources which appear point like in the image processed IRAS maps at 60 & 100 μm, have been resolved into either multiple components or found to be extended in the TIFR maps (Ghosh et al. 1996, Ghosh 1998, Karnik et al. 1999a, Mookerjea et al. 1999b, Verma et al. 1999a). Reliable dust temperature and optical depth maps have been produced for the extended source RAFGL 5111 (Mookerjea et al. 1999a). The Galactic plane survey maps

($l \approx 333°$, $b \approx -0.5°$) have led to interesting information about star forming activity in that region (Karnik et al 1999b). Several other studies of the SFRs listed in Table 1, are in progress. Three SFRs (IRAS 19181+1349, 20178+4046 & 20286+4105) were selected for MIR observations, on the basis of their interesting SED and / or FIR morphology. They were observed in 7 bands (3.3, 3.7, 6.0, 6.7, 7.7, 9.6 & 11.4 μm) using the ISOCAM instrument on board the Infrared Space Observatory (ISO). These bands cover 4 features of the newly discovered ubiquitous component of the interstellar matter, viz., Polycyclic Aromatic Hydrocarbons (PAH). The other 3 bands quantify the neighbouring continua. Surprisingly, the isophots for the MIR bands (continua as well as the PAH features) resemble the FIR maps very closely. Excess emission in the PAH features, over the underlying continua have been clearly detected for all these 3 sources (Verma et al 1999a).

Table 1. Galactic star forming regions mapped in two far infrared bands using the 12 channel photometer system

IRAS PSC name	Other name	Area mapped	Date of observation DD/MM/YYYY
Outflow sources			
00338+6312	L 1287	22' × 07'	12/11/1995
00494+5617	NGC 281W	22' × 12'	12/11/1995
01195+6136	S 187	32' × 26'	12/11/1995
05391–0217	NGC 2023	46' × 38'	12/11/1995
Ultra Compact / Compact H II regions			
02232+6138	W 3 (OH)	29' × 20'	18/11/1993
18507+0121		32' × 24'	20/02/1994
19181+1349		32' × 24'	20/02/1994
20178+4046		32' × 24'	20/02/1994
20255+3712	S 106	32' × 24'	20/02/1994
Galactic Plane Survey ($l = 333°$; $b = -0.5°$)			
	RCW 106 complex	2215 sq. arc min total	
16164–5046			20/02/1994
16167–5034			20/02/1994
16172–5028			20/02/1994
16177–5018	G333.292		20/02/1994

Table 1. Continued

IRAS PSC name	Other name	Area mapped	Date of observation DD/MM/YYYY
H II region / Molecular clouds			
03595+5110	RAFGL 5111	24' × 11'	12/11/1995
04073+5102	RAFGL 550	23' × 13'	12/11/1995
05327–0457	NGC 1977	43' × 34'	12/11/1995
05387–0149	H-H 67	44' × 28'	12/11/1995
09002–4732	G268.454	29' × 20'	18/11/1993
09227–5146	RCW 42	29' × 20'	18/11/1993
10049–5657	RAFGL 4101	32' × 20'	20/02/1994
12127–6244	RAFGL 4148	32' × 26'	08/03/1998
12320–6122	G300.956	32' × 29'	08/03/1998
12326–6245		32' × 26'	08/03/1998
14416–5937		32' × 20'	20/02/1994
15015–5720	RCW 87	29' × 25'	08/03/1998
16571–4029	RCW 116B	32' × 24'	20/02/1994
17009–4042	G345.495	30' × 24'	08/03/1998
17059–4132	G345.425	32' × 30'	08/03/1998
17160–3707		31' × 24'	08/03/1998
17233–3606		28' × 24'	08/03/1998
19111+1048	RAFGL 2341	30' × 26'	08/03/1998
19201+1400	Bonn 48.997	31' × 27'	08/03/1998
19207+1410	Bonn 49.204	32' × 26'	08/03/1998
19209+1421	Bonn 49.384	31' × 37'	08/03/1998
20286+4105		32' × 24'	20/02/1994

2. Radiative transfer modelling

Several distinct radiative transfer schemes have been developed / used to model embedded young star / (s) or cluster / (s) in an interstellar cloud. They consider either one (spherical geometry) or two (cylindrical geometry) embedded source / (s) of energy. In one of the schemes, in addition to the emission and absorption processes of dust grains in thermal equilibrium, the non-equilibrium processes have also been included. The latter are important for Very Small Grains (VSG) and the PAH, since their internal energy is smaller than or comparable to the energy of individual UV photons. The models are constrained by all available measurements relevant to continuum emission from the dust (infrared; sub-mm) and the gas (radio continuum), occasionally supplemented by the data in spectral features as well (due to dust; PAH; fine structure lines of heavy elements in the interstellar gas; etc). For a particular SFR under study, the model that fits the observed SED and the radial intensity profiles (at different wavelengths) the best, leads to the determination of the following details about that SFR : nature of the

exciting source / (s), physical dimensions of the cloud, radial density distribution, dust to gas ratio, dust composition etc.

2.1 Spherical geometry

A self-consistent radiative transfer scheme has been developed which considers the dust as well as the gas components. Self-consistency implies that the same geometric and physical configuration fits the observed data for the emission from the dust (most of the infrared, sub-mm, mm part of the SED) as well as the emission from the gas (radio continuum, fine-structure line intensities etc). Two kinds of dust have been considered (Draine & Lee 1984 (DL); and Mathis et. al., 1983 (MMP)), each with its own variable composition. Various geometric and physical details of the SFRs are determined from this modelling scheme.

In order to assess the effectiveness of this scheme, three young Galactic star forming regions associated with IRAS 18314 –0720, 18355–0532 and 18316–0602 have been modelled as test cases (Mookerjea & Ghosh 1998). They cover a large range of luminosity (≈ 40). Interestingly, in all these three cases, the best fit models correspond to the uniform density distribution (for either DL or MMP dust!). For both IRAS 18314–0720 as well as 18355–0532, although both the DL as well as MMP dust lead to acceptable fits to the infrared SED (corresponding to identical optical depth), the radio continuum data is better predicted by the latter. The quality of fit to the SED is however always superior for the DL case than MMP (see Fig. 1). In the case of IRAS 18316–0602, DL is the preferred model since not only it gives a better fit to the observed SED, it also predicts radio continuum consistent with the measurements. Whereas, the most favoured dust composition by mass (in the DL case) for IRAS 18314–0720 & 18355–0532 is mainly equal mixture of graphite & silicon carbide with traces (≈ 5–7%) of silicate, the same for IRAS 18316–0602 is mostly (72%) silicate grains with the rest being graphite.

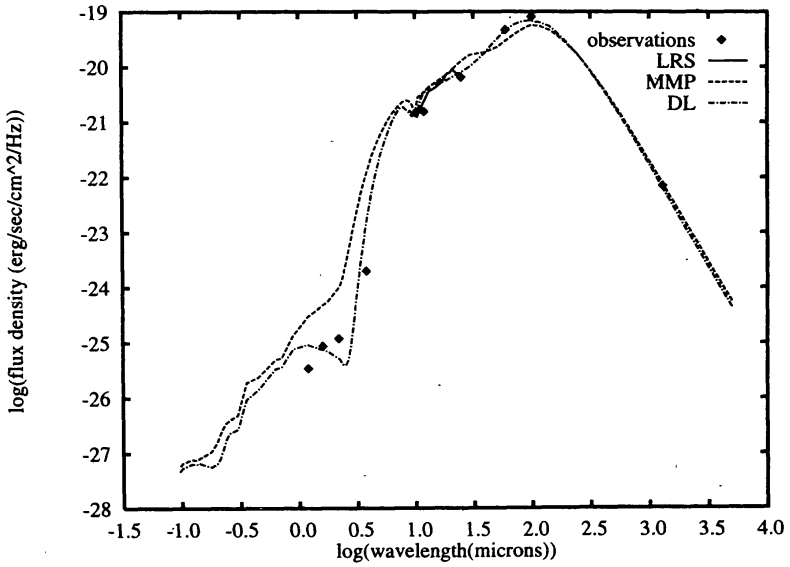

Figure 1. The spectral energy distribution for the source IRAS 18314-0720. The solid line represents IRAS LRS observations; the dashed line represents model with MMP grains, the dash-dot-dash line represents model with DL grains. The diamond symbol represents other observations.

2.2 Cylindrical geometry : two embedded sources

High angular resolution mid / far infrared maps of many Galactic star forming regions show evidence for multiple embedded energy sources in the corresponding interstellar clouds. With the aim of studying such star forming regions with two embedded sources, a radiative transfer scheme has been developed (Karnik & Ghosh 1999). This scheme, CYL2S, carries out radiative transfer calculations through the uniform density dust component in a cylindrical geometry, and includes the effect of isotropic scattering in addition to the absorption and emission processes. The axis of the cylinder is taken along the line joining the two embedded protostars / young stars. In addition to the luminosities of the two embedded energy sources, the cylindrical cloud size, separation between the two sources, dust density, dust size distribution & composition are the parameters for the modelling. This code has been quantitatively validated by simulating the case of a single embedded source and comparing results from another accurate code dealing with the spherically symmetric geometry (CSDUST3; Egan et. al. 1988).

In order to demonstrate the usefulness of our code, an attempt is made to model the Galactic star forming region associated with IRAS 19181+1349 which shows two peaks in the mid & far infrared maps (Verma et. al. 1999b). Two independent approaches have been employed to find the best fit models for IRAS 19181+1349. Whereas the first (M_{SED}) approach aims to fit the observed SED best; the latter (M_{RC}) aims to fit the radial intensity profiles (along a few important axes) at mid to far infrared wavebands (see Fig. 2). Interestingly the most of the crucial model parameters like luminosities, effective temperatures, dust composition, optical depth etc turn out to be identical under both the approaches (Karnik & Ghosh 1999). This demonstrates our CYL2S scheme to be a very useful tool for studying Galactic star forming regions with multiple embedded sources.

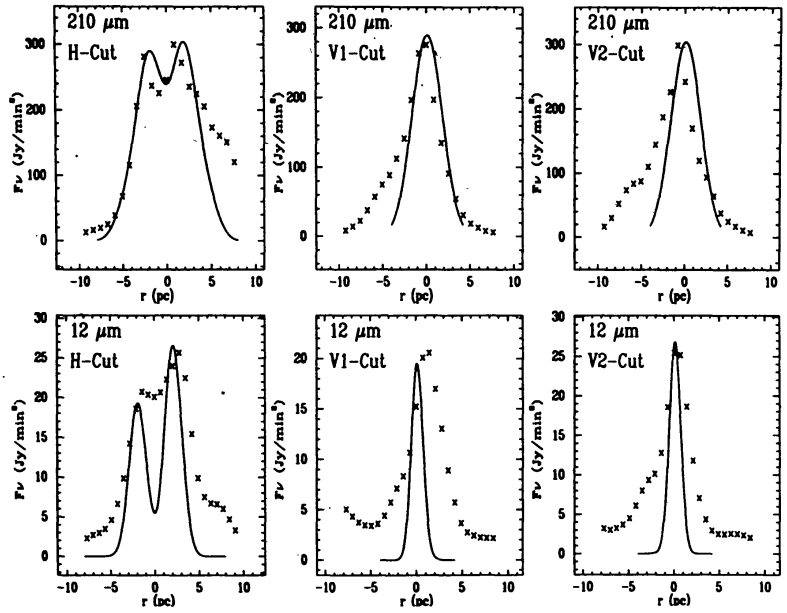

Figure 2. The axial (H) and radial (V1 & V2) cuts predicted by the radiative transfer model M_{RC} (continuous lines), compared with the observations (crosses) of IRAS 19181+1349 at 12 and 210 μm.

2.3 Transient heating of the VSG & the PAH

In a typical SFR environment, the temperatures of the VSG and the PAH components fluctuate, because their enthalpy is comparable to the energy of a single UV / optical photon. Hence, the multiphoton absorption processes lead to a modification to their temperature distribution. An interactive method has been used to consider these multiphoton processes (Ghosh & Verma 1999). The method assumes a single grain in an isotropic radiation field and follows the evolution of the grain temperature by solving the relevant stochastic differential equation (Desert et. al. 1986).

The spherically symmetric dust cloud, containing the embedded energy source is divided into a large number of concentric contiguous spherical shells like "onion skins". Two kinds of grains have been incorporated : (i) the normal grains (Big Grains, BG, mainly responsible for thermal emission) (ii) the grains for which the non-equilibrium processes are important (VSG & PAH). Each shell has been subdivided into a pair of sub-shells corresponding to these two components (see Fig. 3) Radiative transport at each of the two sub-shells is carried out as a two point boundary value problem, the two boundary conditions being the incident radiation fields at the two surfaces. The radiative transport through the sub-shells consisting only of the normal grains, (Sh^{BG}), has been carried out using the code CSDUST3 developed by Egan et. al. (1998). Starting from the inner most shell, the radiation is transported through the successive shells, till the outer boundary of the cloud is reached. This entire processing is repeated till the necessary convergence is achieved.

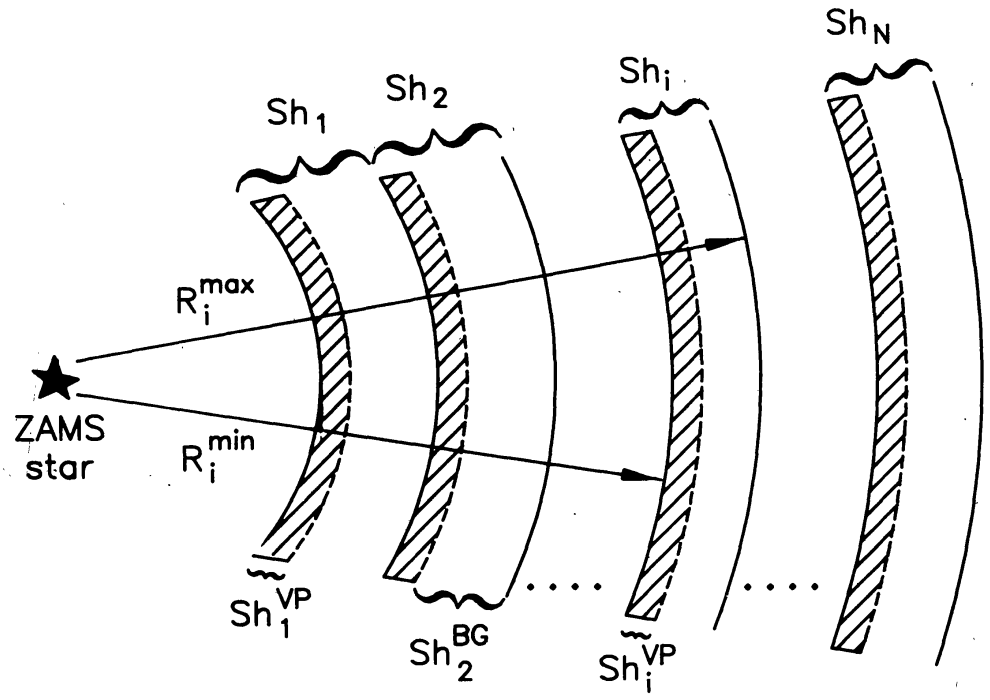

Figure 3. The schematic diagram of "onion skin" shell structure of the interstellar cloud with an embedded star. The sub-shells Sh^{BG} consist only of normal grains (BG), and the sub-shells Sh^{VP} consist only of VSG & PAH.

A sample of five Galactic compact H II regions (IRAS 18116-1646, 18162-2048, 18434-0242, 19442+2427 & 22308+5812), for which high resolution mid infrared spectroscopic data are available (Roelfsema et. al. 1996), have been chosen for detailed modelling using the above scheme. In addition to the ISO-SWS data, the IRAS PSC measurements, the IRAS LRS spectra and other available ground based near infrared photometric / spectroscopic data have also been used.

The VSG component is taken to be graphite grains of a single size : either 10 Å or 50 Å in radius. The scattering and absorption coefficients for the VSG have been taken from Draine & Lee (1984) and Laor & Draine (1993). The PAH component is assumed to be either a single molecule with about 15 - 30 atoms, or a large complex consisting of 10 - 20 small molecules as used by Siebenmorgen (1993). Their optical properties have been taken from Leger & d'Hendecourt (1987).

The best fit model spectrum for the compact H II region IRAS 18162-2048 is compared with observations in Figure 4. The most favoured radial dust density distribution law, for all five sources, turns out to be of uniform density. In order to reproduce the spectral features of PAH, it is necessary that the PAH component is confined only to a thin central shell whose thickness is just a few percent (1.3 - 5.5%) of the total thickness of the dust cloud. The normal big grains are dominated by graphites, with silicates contributing less than 25%.

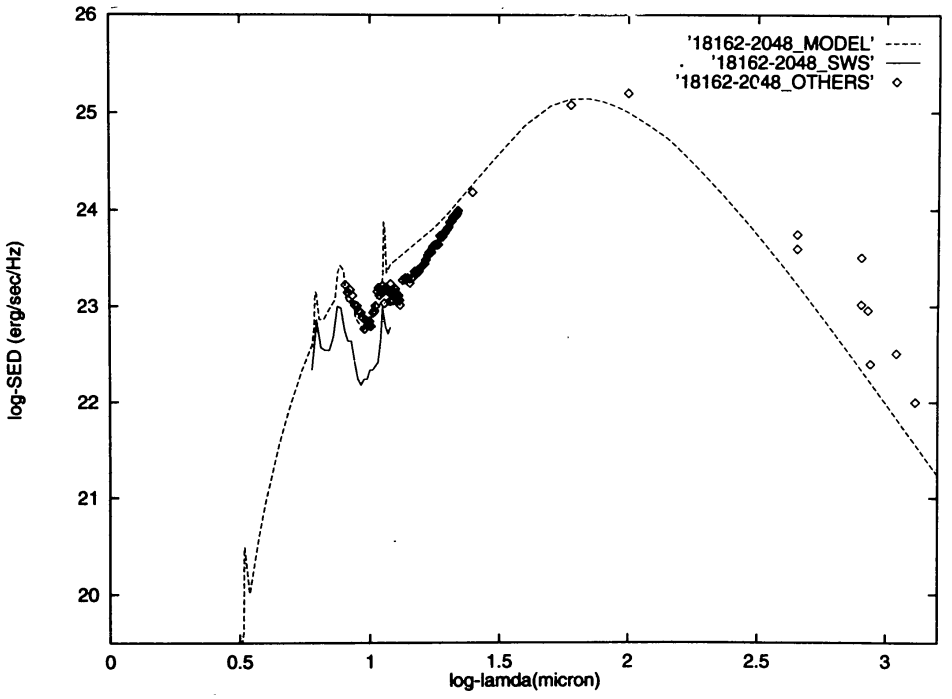

Figure 4. Spectral energy distribution of the compact H II region IRAS 18162-2048. The solid line shows the ISO-SWS spectrum from Roelfsema et al. (1996); dotted line shows our best fit model spectrum; and the diamonds show other observations.

Acknowledgements

The studies reviewed here have been carried out in collaboration with one or many of my following colleagues : A. D. Karnik, B. Mookerjea, T. N. Rengarajan, S. N. Tandon & R. P. Verma. It is a pleasure to acknowledge their contributions, and thank them for the same. Thanks are also due to S. L. D'Costa, M. V. Naik, D. M. Patkar, M. B. Naik and other members of the Infrared Astronomy group of TIFR for their scientific & technical support.

References

Desert F. X., Boulanger F., Shore S. N., 1986, A&A, 160, 295.

Draine B. T., Lee H. M., 1984, ApJ, 285, 89.

Egan M. P., Leung C.M., Spagna G. F., 1988, Computer Physics Communications, 48, 271.

Ghosh S. K., 1998, in "Perspectives in High Energy Astronomy & Astrophysics", eds. P. C. Agrawal, P. R. Vishwanath, Universities Press, P. 268.

Ghosh S. K., Iyengar K. V. K., Rengarajan T. N., Tandon S. N., Verma R. P., Daniel R. R., 1988, ApJ, 330, 928.

Ghosh S. K., Rengarajan T. N., Verma R. P., Karnik A. D., 1996, in "Interplay between Massive Star Formation, the ISM and Galaxy Evolution", eds. D. Kunth, B. Guiderdoni, M. Heydari-Malayeri, T. X. Thuan, p. 499.

Ghosh S. K., Verma R. P., 1999, (submitted)

Karnik A. D., Ghosh S. K., 1999, (Submitted)

Karnik A. D., Ghosh S. K., Rengarajan T. N., Tandon S. N., Verma R. P., 1999a, BASI, 27, 167.

Karnik A. D. et al., 1999b, (in preparation).

Laor A., Draine B. T., 1993, ApJ, 402, 441.

Leger A., d'Hendecourt L., 1987, in "PAH and Astrophysics", eds. A. Leger, L. d'Hendecourt, N. Boccara, p. 223.

Mathis J. S., Mezger P. G., Panagia N., 1983, A&A, 128, 212.

Mookerjea B., Ghosh S. K., 1998, (submitted).

Mookerjea B., Ghosh S. K., Karnik A. D., Rengarajan T. N., Tandon S. N., Verma R. P., 1999a, Ap. J., in press.

Mookerjea B., Ghosh S. K., Karnik A. D., Rengarajan T. N., Tandon S. N., Verma R. P., 1999b, BASI, 27, 155.

Roelfsema P. R., Cox P., Tielens A. G. G. M. et al., 1996, A&A, 315, L289.

Siebenmorgen R., 1993, ApJ, 408, 218.

Verma R. P., Ghosh S. K., Karnik A. D., Mookerjea B., RengarajanT. N., 1999a, BASI, 27, 159.

Verma R. P., Ghosh S. K., Karnik A. D., Mookerjea B., Rengarajan T. N., 1999b, in "The Universe as seen by ISO", ed. P. Cox, ESA Special Publication SP-427, (in press).

Verma R. P., Rengarajan T. N., Ghosh S. K., 1993, BASI, 21, 489.